Reduced-Reference Image Quality Assessment via Intra- and Inter-Subband Statistical Characteristics in Reorganized DCT Domain

Lin Ma, Songnan Li, and King N. Ngan
Department of Electronic Engineering, The Chinese University of Hong Kong, Hong Kong
E-mail: {lma, snli, knngan}@ee.cuhk.edu.hk, Tel: +852-26098251

***Abstract*— In this paper, a novel reduced-reference (RR) image quality assessment (IQA) is proposed by depicting the intra- and inter-subband statistical characteristics in the reorganized discrete cosine transform (DCT) domain. Firstly, the block-based DCT coefficients are reorganized into a three-level tree. Generalized Gaussian density (GGD) function is employed to capture the intra-subband characteristics. The difference between the actual coefficient distribution and GGD is depicted by city-block distance (CBD). For the inter-subband characteristics, the mutual information (MI) between adjacent reorganized DCT subbands is utilized to depict the corresponding relationships. By combining the CBD of intra-subband and the MI of inter-subband together, the proposed RR IQA is developed. Experimental results demonstrate that compared to existing methods a smaller number of RR features is required for representing the image perceptual quality. The proposed method outperforms the RR WNISM and FR PSNR, and performs comparably with the FR SSIM.**

I. INTRODUCTION

Image visual quality measurement is becoming a more and more important issue, especially due to the multimedia content transmission over the Internet. It is very useful for various image processing applications, such as image communication, compression, printing, display, registration, restoration, enhancement, and so on [1]. As human eyes are the ultimate receivers of the images/videos, the subjective testing method is the most reliable for evaluating the image/video visual quality. However, the subjective testing method [2] requires many observers to participate in the experiments and provide their personal opinions of the image/video quality. It is very time-consuming and expensive, which cannot be employed for the practical image/video applications. Consequently, the image/video quality metrics [3] which can automatically assess image/video visual quality are desired.

According to the availability of the reference image, there is a general agreement [3] that the quality metric can be categorized into three classes: full-reference (FR) [5]-[9], no-reference (NR) [10]-[14], and reduced-reference (RR) [15]-[26]. The FR quality metric requires the whole reference image to evaluate the visual quality of the distorted one, which can be utilized in image/video compression, watermarking, and so on. Mean square error (MSE) and the corresponding peak signal-to-noise ratio (PSNR) are the most widely utilized FR metrics, for the simple formulation, easy optimization and clear physical meaning. However, many researchers have doubted the effectiveness of MSE/PSNR for modeling the image/video perceptual quality [4]-[26], as their performances correlate poorly with the subjective ratings of the viewers. In order to handle the drawbacks of MSE/PSNR, Wang et al. [5] proposed the famous structure similarity (SSIM) index to depict the structural distortions rather than the pixel absolute differences. Ma et al. [8] proposed to incorporate the orientation sensitivity and conspicuity of the human visual system (HVS) into SSIM to derive a more accurate image quality assessment (IQA). Recently, Chandler et al. [6] derived the IQA to depict the visual signal-to-noise ratio (VSNR) in the wavelet domain. However, these IQAs are too complicated to be optimized for image coding. Accordingly, Zhang et al. [9] simply considered the contrast sensitivity function and contrast masking effect of the HVS to develop a simple image quality metric, which has been proved to be effective for image compression.

However, in many practical applications, the reference image is not available, such as image denoising, restoration, and super-resolution. The NR IQAs [11] are thus very important to control the visual quality of the final processed images. It is an extremely difficult task. Therefore, many researchers take the behaviors of specific distortions into consideration. As JPEG 2000 encodes the image in the wavelet domain, the wavelet statistical model is employed to capture the distortion introduced by JPEG 2000 in [10]. Liang et al. combined the sharpness, blurring, and ringing metrics together to evaluate the visual quality of the JPEG 2000 coded image. And Brandao et al. [13] proposed an NR IQA based on the DCT domain statistics to evaluate the quality of JPEG coded image. Furthermore, Ferzli el al. [14] have done the psychophysical experiments to test the blur tolerance ability of the HVS, which is denoted as Just-Noticeable Blur (JNB). However, the properties and behaviors of the distortions are independent of each other. The prior knowledge of all the distortions is hard to learn for depicting the image visual quality. Therefore, in order to provide a compromise between FR and NR IQA, RR methods have been developed for IQA

by employing some partial information of the corresponding reference image. With a limited amount of information extracted from the reference image, the RR methods can efficiently evaluate the image quality. As only a small number of bits are required for representing the extracted features, it can be easily coded and transmitted with the images/videos. Consequently, it will be very useful for the quality monitoring during the image/video transmission and communication. Based on the features embedded in the transmitted images/videos, we can easily assess the corresponding real-time visual quality. Based on the quality monitoring, we can provide a better quality of experience for the consumers.

For the RR IQAs, Wang et al. [23] [24] proposed a wavelet-domain natural image statistic metric (WNISM), which tries to model the marginal probability distribution of the wavelet coefficients of a natural image by using the generalized Gaussian density (GGD) function. Then the Kullback-Leibler distance (KLD) is used to calculate the distribution difference, representing the perceptual quality of the distorted image. Although WNISM achieves good performances on the image quality assessment, some limitations can still be figured out. Firstly, the KLD is asymmetric [27]. As demonstrated in [26], it is not suitable for image quality assessment, because the visual quality distance from one image to another should be identical no matter how it is measured. Secondly, as revealed by [25], although WNISM can work quite well on individual distortion types, its performance degrades significantly when images with different distortion types are evaluated together. Therefore, in order to handle these problems, Ma et al. [26] proposed an RR IQA by using the reorganized DCT-based image representation. The DCT coefficients are firstly reorganized into several representative subbands. GGD is employed to model the distribution of each subband. The city-block distance (CBD) is used to depict the distribution differences. Although a better performance has been achieved by [26], only the identical nature of the coefficient distributions in the same reorganized subband is utilized for the design of the RR IQA. However, the correlations between inter-reorganized DCT subbands do also exist and may be helpful for image quality assessment. To the best of our knowledge, all the image statistical modeling based RR IQAs [23]-[26] do not consider the inter-subband correlations.

In this paper, a novel perceptual RR IQA is developed by depicting both the intra- and inter-subband statistical characteristics in the reorganized discrete cosine transform (DCT) domain. With the reorganization strategy, the identical natural of the coefficient distribution within the reorganized subband is utilized. Furthermore, it is demonstrated by experiments that the inter-subband relationship is also very important for assessing the image visual quality. Therefore, by considering both the intra- and inter-correlation of the subbands, an efficient RR IQA is finally developed.

This paper is organized as follows. Section II presents the detailed algorithm of our proposed RR IQA. Section III demonstrates the performance comparisons. Finally, the conclusion is given in Section IV.

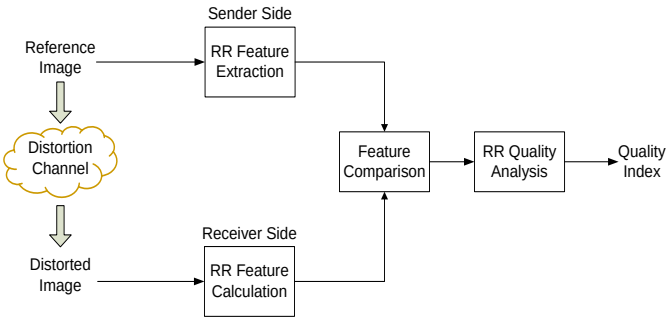

Figure 1. General framework of the RR IQA system

II. The Proposed Reduced-Reference Image Quality Metric

The general framework of the RR IQA is illustrated in Figure 1. After capturing, storing, and such processes, some distortions have been introduced into the reference image, which can be modeled as the distortion channel. As mentioned before, with the limited amount of information about the reference image, the RR IQA is required. In order to develop an efficient RR IQA, several challenges need to be handled. In the sender side, we need to extract several features which are sensitive to a variety of image distortions. Also they need to be relevant to the visual perception of the image quality. Then the RR extracted features can be embedded in the image or transmitted to the receiver side for further quality analysis. Another important aspect is that the RR feature selection should consider not only the prediction accuracy of the image quality, but also the data rate of the RR features. For a higher data rate, one may include much more information about the reference image. Then a good performance can be obtained, which will introduce a heavy burden to the RR feature transmission. Actually, the FR IQA is the extreme case of RR IQA, with the data rate is the whole reference image. While for a smaller data rate, only a little information is available, the quality prediction accuracy is hard to be insured. The NR IQA is also the extreme case of RR IQA, with no information from the reference image. How to balance the data rate and performance is the key point for RR feature selection. In the receiver side, some features related to the distorted image are calculated. By comparing the features from the sender and receiver side, we can analyze how much degradations have been introduced into the distorted image. Finally, the visual quality index is generated.

A. Reorganization Strategy of DCT Coefficients

As DCT has been widely employed in the image/video compression standards, such as JPEG, MPEG2, and H.264, the image statistics in DCT domain can easily capture the differences between the distorted image and the original one. That's also one of the reason why DCT is considered in [26] other than steerable pyramid in [23] [24]. As the RR IQA needs to balance between the accuracy of image quality assessment and the data rate of RR features, the reorganization strategy [26] [28] [29] is employed for composing the block-based DCT coefficients into a three-

level tree structure, as demonstrated in Figure 2. Firstly, the 8×8 DCT is performed block by block on the image. The 8×8 DCT coefficients of each block are decomposed into ten subbands. By grouping and organizing the DCT coefficients together according to their corresponding positions, the whole image is reorganized into a three-level coefficient tree. In Figure 2, S_n denotes the grouped subband of all the DCT coefficients lying on the position denoted by n.

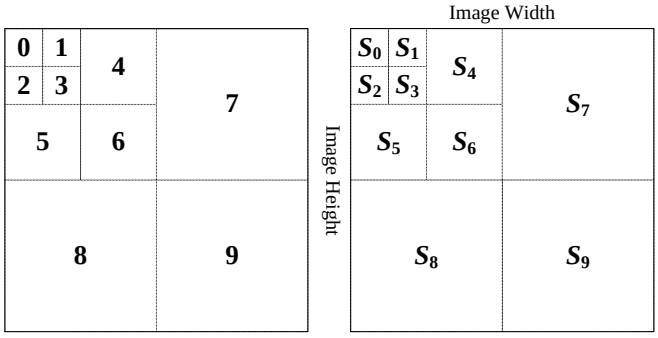

Figure 2. Reorganization strategy of DCT coefficients (Left: one 8×8 DCT block with ten subband decomposition; right: the reorganized DCT image representation taken as a three-level coefficient tree)

B. RR Feature Extraction in the Sender Side

Figure **3** provides the framework for extracting the RR features from the reference image. As shown in the figure, not only the dependencies of intra reorganized DCT subbands, but also the dependencies of inter reorganized DCT subbands exist, which we divide into inter-scale and intra-scale. As shown in [26], the intra-subband correlations, which have been proved to be sensitive to the image distortion, can be utilized for the RR IQA. The identical nature of the coefficient distributions between adjacent DCT subbands in the same reorganized DCT subband is employed for extracting the useful RR features. The generalized Gaussian density (GGD) is employed to depict the coefficient distribution in each reorganized DCT subband:

$$p_{\alpha,\beta}(x) = \frac{\beta}{2\alpha\Gamma\left(\frac{1}{\beta}\right)} e^{-\left(\frac{|x|}{\alpha}\right)^{\beta}} \tag{1}$$

where $\beta > 0$ and α are two parameters of the GGD function. Γ is the Gamma function given by

$$\Gamma(x) = \int_0^{\infty} t^{x-1} e^{-t} dt \tag{2}$$

Here α models the width of the PDF peak (standard deviation), while β is inversely proportional to the decreasing rate of the peak. Also α and β are referred to as the scale and shape parameters, respectively. As demonstrated in [26], GGD is more suitable for modeling the coefficient distribution in the reorganized DCT domain, which results in a better performance of the RR IQA. Moreover, by considering the maximum-likelihood estimation and assuming $\beta > 0$, we can obtain the approximated $\hat{\alpha}$ [34] according to:

$$\hat{\alpha} = \left(\frac{\beta}{L}\sum_{i=1}^{L}|x_i|^{\beta}\right)^{\frac{1}{\beta}} \tag{3}$$

where x_i is the coefficient sample from the corresponding reorganized DCT subband, L denotes the total number of the coefficients. From (3), it can be observed that the estimated $\hat{\alpha}$ is highly related to the subband energy in the β-norm. And the subband energy can somewhat reflect the level of the image distortion. That is the reason why we introduce GGD to model the coefficient distribution, not only because of the modeling accuracy but also the reflection of the subband energy. Furthermore, another parameter besides (α, β) is employed for improving the modeling accuracy, which is named as the city-block distance (CBD) [26]:

$$d_{CBD}(p, p_{\alpha,\beta}) = \sum_{i=1}^{h_L}\left|p(i) - p_{\alpha,\beta}(i)\right| \tag{4}$$

where $p(i)$ is the histogram of the actual reorganized DCT subband, $p_{\alpha,\beta}(i)$ is the fitted GGD histogram, and h_L is the total number of the histogram bins. Compared with KLD, CBD is symmetrical, which is more reasonable for evaluating image visual quality.

For the inter-subband relationships, the dependencies are depicted by the mutual information (MI), which can be expressed as:

$$\begin{aligned} I(X;Y) &= h(X) - h(X|Y) \\ &= E_X(-log_2\, p(x)) - E_{X,Y}(-log_2\, p(x|y)) \end{aligned} \tag{5}$$

where $h(X)$ and $h(X|Y)$ denote the entropy of X and X conditioned on Y. As shown in (5), we can observe that the MI is symmetric and non-negative. If X and Y are independent, the MI is equal to zero. Actually, the MI $I(X;Y)$ indicates how much information Y conveys about X. Actually, it admits a well-know data compression interpretation: coding X to a precision ΔX costs $h(X) - log_2(\Delta X)$ bits, based on the assumption that ΔX is sufficiently small. If Y is known, by considering the same encoding precision ΔX, the total bits cost for encoding X is equal to $h(X) - log_2(\Delta X) - I(X;Y)$ bits [27]. Therefore, the total saving bits by introducing Y is $I(X;Y)$.

For the reorganized DCT subbands, the MI is employed to depict the inter-scale relationship. Similar to wavelet representation, one parent DCT coefficient corresponds to four DCT coefficients in the reorganized child DCT subband. Therefore, we firstly interpolate the parent DCT subband into the same size of the reorganized child DCT subband through nearest interpolation process. It means that we copy one DCT coefficient into a 2×2 coefficient matrix with the same value. Then after vectorization, the dimensions of the parent and the child subband are the same. Therefore, the corresponding MI value can be calculated.

To the distorted image whose visual quality is to be evaluated, the DCT coefficients will be corrupted by the corresponding distortions. Meanwhile the relationship

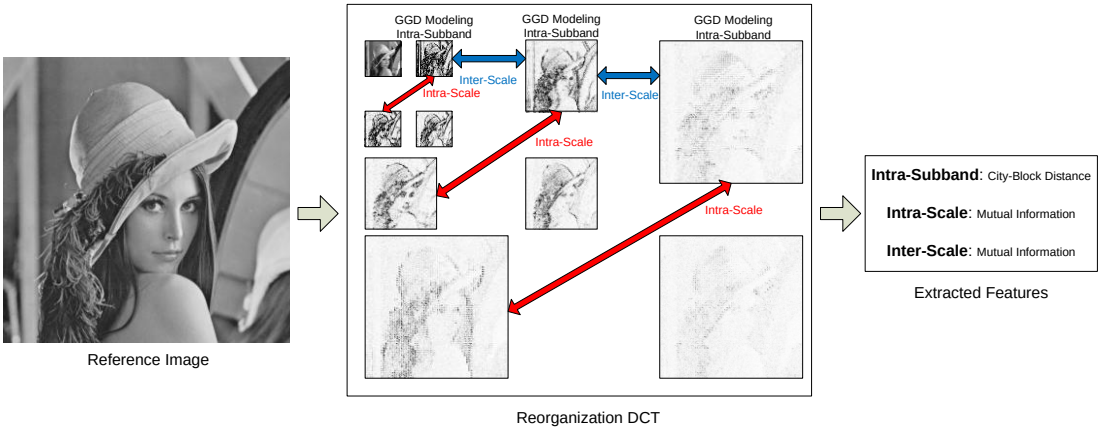

Figure 3. Feature Extraction in the Sender Side

between the DCT coefficients will be changed. For the reason of a limited number of RR features, it is not practical to compare the differences between the DCT coefficients. In order to depict the distortion level then evaluate the visual quality, the MI value is introduced in the sender side to describe the essential relationship between the inter reorganized DCT subbands. The extracted MI values together with the GGD parameters can be embedded into the image and transmitted to the receiver side for the final RR feature comparison and visual quality analysis.

C. Visual Quality Analysis in the Receive Side

In the receiver side, as shown in Figure **3**, we need to compare the extracted features. Then the visual quality of the distorted image is analyzed giving the final visual quality index. For the intra-reorganized DCT subband, CBD is employed to depict the distance between the reference image and the distorted one:

$$d_{CBD}(p, p_d) = \sum_{i=1}^{h_L} |p(i) - p_d(i)| \tag{6}$$

where p is the coefficient distribution of the reference image, and p_d is the corresponding distorted one. However, as the reference image is not available in the receiver side, the lower bound is introduced for approximating the distance:

$$d_{CBD}(p, p_d) \triangleq d_{CBD}(p, p_{\alpha,\beta}) - d_{CBD}(p_{\alpha,\beta}, p_d) \tag{7}$$

where $d_{CBD}(p, p_{\alpha,\beta})$ is the third parameter introduced in the sender side. Therefore, in the receiver side, only $d_{CBD}(p_{\alpha,\beta}, p_d)$ needs to be calculated. Their difference will be recorded to represent the statistical feature distance of the intra-subband.

For the inter-reorganized DCT subbands, the MI values are calculated. The MI between subbands of adjacent scales will be extracted as the inter-scale feature, while the MI between subbands in the same scale is extracted as the intra-scale feature. For the distorted image in the receiver side, the difference between the MI values is measured as:

$$d_{MI}(S_m, S_n) \triangleq I(S_m, S_n) - \hat{I}(S_m, S_n) \tag{8}$$

where $I(S_m, S_n)$ is the MI of the reorganized DCT subbands S_m and S_n of the reference image, and $\hat{I}(S_m, S_n)$ is the MI of the corresponding subbands of the distorted image.

By accounting for the difference of CBD and MI over the denoted subbands, the final visual quality index can be generated:

$$V_q = log_{10}\left(1 + \frac{\lambda \times \sum_{Sub} d_{CBD}(p, p_d) + \sum_{Sub} d_{MI}(S_m, S_n)}{c}\right) \tag{9}$$

where Sub denotes the reorganized DCT subbands to be included, λ is an introduced parameter which simply balances the contribution of CBD and MI to the final visual quality score V_q. In this paper, λ is set as 5. c is utilized for scaling the distortion measure to avoid the variation of V_q being too small. As a scaling factor, the parameter c will not influence the performance of the proposed RR IQA, which is set as 0.0001 for simplicity.

III. Experimental Results

In this section, the performances of different IQAs are compared to demonstrate the efficiency of the proposed RR IQA for evaluating the image perceptual quality.

We compare the performance of our proposed RR IQA with the representative RR image quality metric WNISM [23] [24], recently developed RR IQA [26], and the FR metrics: PSNR, and SSIM [5]. The LIVE image database [32] is employed for evaluating the performances of the metrics. The most prevailing distortion types have been considered in the LIVE image database, including JPEG, JPEG 2000, blur, white Gaussian noise (WGN), and fast fading (FF). Each distorted image is assigned a subjective score, specifically the differential mean opinion score (DMOS), which is obtained from subjective viewing tests where many observers participated and provided their opinions on the visual quality of each distorted image. Therefore, it can be regarded as the ground truth for evaluating the metric performances. We follow the performance evaluation procedure introduced in the video quality experts group (VQEG) HDTV test [35] and

that in [36]. Let x_j represent the visual quality index of the jth distorted image obtained from the corresponding IQA. The five parameter logistic function is employed to map x_j into V_j:

$$V_j = \beta_1 \times \left(0.5 - \frac{1}{1 + e^{\beta_2 \times (x_j - \beta_3)}}\right) + \beta_4 \times x_j + \beta_5 \quad (10)$$

The corresponding five parameters $\{\beta_1, \beta_2, \beta_3, \beta_4, \beta_5\}$ are determined by minimizing the sum squared differences between the mapped objecting scores V_j and the subjective DMOS values. In order to evaluate the performances, three statistical measures are employed: linear correlation coefficient (LCC), Spearman rank-order correlation coefficients (SROCC), and root mean square prediction error (RMSE). According to the definitions, larger values of LCC and SROCC mean that the objective and subjective scores correlate better, that is to say, a better performance of the IQA. And smaller RMSE values indicate smaller errors between the two scores, therefore a better performance.

As the RR IQA tries to balance between the RR data rates and the quality prediction accuracy, we will not introduce all the reorganized DCT subbands and their corresponding relationships for extracting the RR features. As discussed in [26], a smaller number of the reorganized DCT subbands can provide a good performance. And according to the oblique effect [33] of the HVS, human eyes present similar sensitive value to the horizontal and vertical information, while less sensitive to the diagonal information. Therefore, in order to reduce the RR data rates, only three horizontal reorganized DCT subbands are accounted for. As three parameters $\{\alpha, \beta, d_{CBD}(p, p_{\alpha,\beta})\}$ are utilized for depicting the coefficient distribution, $3 \times 3 = 9$ parameters are extracted for the total three horizontal subbands. Meanwhile, only the inter-dependencies related to the horizontal subbands are extracted as the RR features, as illustrated in Figure 3. Therefore, together with the features depicting the intra-subband statistical properties, $9 + 2 + 3 = 14$ parameters in total are extracted for the proposed RR IQA. And the performances of different IQAs are illustrated in Table I. It can be clearly observed that our proposed method can outperform the WNISM, RR IQA [26], and the PSNR, with larger LCC/SROCC and smaller RMSE. Also it performs comparably with the FR SSIM. The scatter-plots of different IQAs are illustrated in Figure 4. It can be observed that the points scatter more closely to the fitted line, which means that the DMOS values correlate better with the visual quality values obtained by the proposed method.

However, SSIM employs the whole reference image for quality assessment. Our proposed method only requires 14 features to represent the reference image, which is even smaller than WNISM [23] [24] and the RR IQA in [26]. For the GGD parameters $\{\alpha, \beta, d_{CBD}(p, p_{\alpha,\beta})\}$, same as [23] [26], these parameters are quantized into finite precision while maintaining a reasonable approximation. Both β and $d_{CBD}(p, p_{\alpha,\beta})$ are quantized into 8-bit precision, and α is represented using 11-bit floating point, with 8 bits for precision and 3 bits for exponent. Therefore, $8 + 8 + 8 + 3 = 27$ bits are needed for each reorganized subband. For the MI values, 8-bit representation is employed. Therefore, for the total 14 features employed in our proposed method, only $27 \times 3 + 2 \times 8 + 3 \times 8 = 121$ bits are needed to represent the extracted RR features.

Table I. Performances of Different IQAs

	PSNR	SSIM	WNISM	RR IQA [26]	Proposed
LCC	0.871	0.904	0.738	0.880	0.905
SROCC	0.876	0.910	0.779	0.876	0.900
RMSE	13.40	11.67	18.43	12.98	11.62

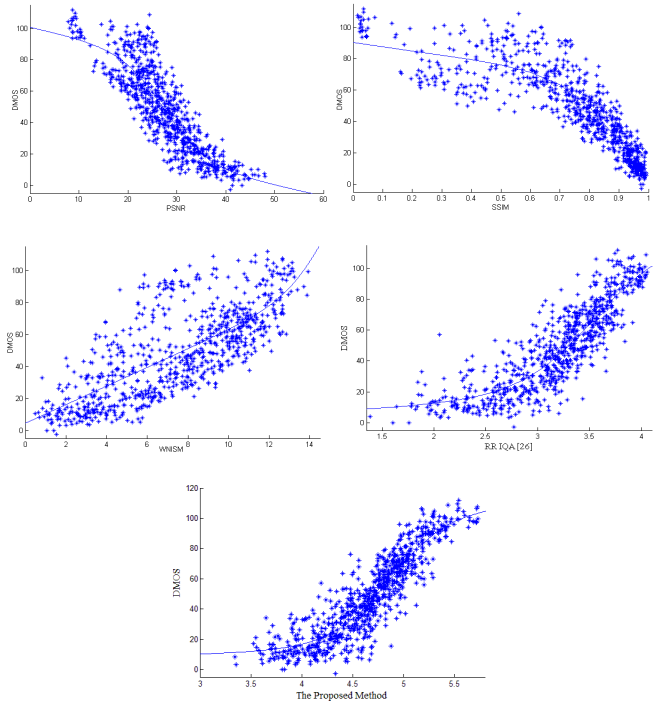

Figure 4. Scatter plots of the DMOS values model predictions on the LIVE image database. Each sample point represents one test image. [Top left: PSNR; top right: SSIM; center left: WNISM; center right: RR IQA [26]; bottom: The proposed method]

Furthermore, we test the proposed RR IQA over individual distortion types from the LIVE image database, which are shown in Table II. It can be shown that our proposed metric outperforms WNISM except for the JPEG 2000 distortion. Actually, JPEG 2000 employed wavelet transform in the encoder. Therefore, the steerable pyramid employed in WNISM is more suitable for depicting the coefficient distribution than the reorganized DCT. Also the proposed metric outperforms the RR IQA [26]. The improvements have demonstrated that the inter reorganized DCT subband correlations, specifically the MI value between reorganized DCT subbands, are helpful for designing the RR IQA. It reflects that the MI values changes between reorganized DCT subbands can somewhat depict the levels of the introduced

distortions. Furthermore, compared to [26], we have reduced the number of RR features for depicting the vertical reorganized DCT subbands. Moreover, although WNISM outperforms PSNR except for the WGN distortion, its performance degrades significantly when image with different types of distortions are tested together, as shown in Table I. As revealed by the previous literature [25], it is also the main drawback of WNISM. For the RR IQA [26] and the proposed method, they can not only perform very well over individual distortions, but also provide a good result over all the distortion types. It means that they are more robust for evaluating image visual quality. And the proposed method performs better than the RR IQA [26], while maintaining a smaller number of RR data rates.

Table II. Performance of Different IQAs Over Individual Distortion Types

		JPEG2000	JPEG	WGN	Blur	FF
PSNR	LCC	0.896	0.887	0.978	0.785	0.891
	SROCC	0.895	0.881	0.985	0.782	0.890
	RMSE	11.22	17.72	8.74	11.45	12.94
WNISM	LCC	0.928	0.862	0.869	0.926	0.918
	SROCC	0.924	0.854	0.848	0.930	0.907
	RMSE	9.37	16.17	13.87	6.96	11.31
RR IQA [26]	LCC	0.846	0.930	0.890	0.931	0.918
	SROCC	0.838	0.924	0.879	0.932	0.911
	RMSE	13.48	11.68	12.70	6.77	11.25
The Proposed Method	LCC	0.882	0.930	0.928	0.939	0.931
	SROCC	0.880	0.925	0.916	0.946	0.915
	RMSE	11.89	11.73	10.45	6.373	10.37

IV. CONCLUSIONS

In this paper, we proposed a novel RR IQA by considering the intra- and inter-subband correlations in the reorganized DCT domain. The CBD and MI values are employed to depict the intra- and inter-subband relationships, respectively. By evaluating on the LIVE image database, the proposed method outperforms WNISM and FR metric PSNR, and performs comparably with the FR metric SSIM. It means that the proposed metric correlates well with the human perception of the image quality. Furthermore, only a small number of RR features are needed to be and transmitted.

REFERENCES

[1] Z. Wang, H. R. Sheihk, and A. C. Bovik, "Objective video quality assessment", in *The Handbook of Video Databases: Design and Application*. Boca Raton. FL: CRC, 2003, pp. 1041-1078.

[2] G. Zhai, J. Cai, W. Lin, X. Yang, W. Zhang, and M. Etoh, "Cross-dimensional perceptual quality assessment for low bit-rate videos", IEEE Trans. Multimedia, vol. 10, no. 7, pp. 1316-1324, Nov. 2008.

[3] Z. Wang, and A. C. Bovik, "Modern image quality assessment". New Youk: Morgan & Claypool, 2006.

[4] B. Girod, "What's wrong with mean-squared error", in Digital Images and Human Vision. Cambridge, MA: MIT Press, pp. 207-220, 1993.

[5] Z. Wang, A. C. Bovik, H. R. Sheihk, and E. P. Simoncelli, "Image quality assessment: from error visibility to structure similarity", IEEE trans. Image Process., vol. 13, no. 4, pp. 600-612, Apr. 2004.

[6] D. M. Chandler, and S. S. Hemami, "VSNR: a wavelet-based visual signal-to-noise ratio for natural images", IEEE Trans. Image Process., vol. 16, no. 9, pp. 2284-2298, 2007.

[7] K. Yang, C. C. Guest, K. E. Maleh, and P. K. Das. "Perceptual temporal quality metric for compressed video", IEEE trans. Multimedia, vol. 9, no.7, pp. 1528-1535, Nov. 2007.

[8] L. Ma, S. Li, and K. N. Ngan, "Visual horizontal effect for image quality assessment", IEEE Signal Process. Letters, vol. 17, no. 7, pp. 627-630, Jul. 2010.

[9] F. Zhang, L. Ma, S. Li, and K. N. Ngan, "Practical image quality metric applied to image coding", IEEE Trans. Multimedia, vol. 13, no. 4, pp. 615-624, Aug. 2011.

[10] H. R. Sheikh, A. C. Bovik, and L. Cormack, "No-reference quality assessment using nature scene statistics: JPEG 2000", IEEE Trans. Image Process., vol. 14, no. 11, pp. 1918-1927, Nov. 2005.

[11] S. S. Hemami, and A. R. Reibman, "No-reference image and video quality estimation: applications and human-motivated design", Signal Processing: Image Communication, vol. 25, no. 7, pp. 469-481, Aug. 2010.

[12] L. Liang, S. Wang, J. Chen, S. Ma, D. Zhao, and W. Gao, "No-reference perceptual image quality metric using gradient profiles for JPEG 2000", Signal Processing: Image Communication, vol. 25, no. 7, pp. 502-516, Aug. 2010.

[13] T. Brandao, and M. P. Queluz, "No-reference image quality assessment based on DCT domain statistics", Signal Processing, vol. 88, no. 4, pp. 822-833, Apr. 2008.

[14] R. Ferzli, L. J. Karam, "A no-Reference objective image sharpness metric based on the notion of just noticeable blur (JNB)", IEEE Trans. Image Process., vol. 18, no. 4, Apr. 2009.

[15] S. Wolf, and M. H. Pinson, "Low bandwidth reduced reference video quality monitoring system", Proc. Int. Workshop Video Process., Quality Metrics for Consumer Electron., Scottsdale, AZ, Jan. 2005.

[16] P. L. Callet, C. V. Gaudin, and D. Barba, "Continuous quality assessment of MPEG2 video with reduced reference", Proc. Int. Workshop Video Process., Quality Metrics for Consumer Electron., Scottsdale, AZ, Jan. 2005.

[17] S. Wolf, and M. H. Pinson, "Spatio-temporal distortion metrics for in-service quality monitoring of any digital video system", Proc. SPIE, vol. 3845, pp. 266-277, 1999.

[18] P. L. Callet, C. V. Gaudin, and D. Barba, "A convolutional neural network approach for objective video quality assessment", IEEE Trans. Neural Netw., vol. 17, no. 5, pp. 1316-1327, May, 2006.

[19] M. Carnec, P. L. Callet, D. Barba, "An image quality assessment method based on perception of structural information", Proc. IEEE Int. Conf. Image Process., vol. 3, pp. 185-188, Sep. 2003.

[20] M. Carnec, P. L. Callet, and D. Barba, "Visual features for image quality assessment with reduced reference", Proc. IEEE Int. Conf. Image Process., vol. 1, pp. 421-424, Sep. 2005.

[21] D. Tao, X. Li, W. Lu, and X. Gao, "Reduced-reference IQA in contourlet domain", IEEE Trans. Syst., Man, and Cybern. B, Cybern., vol. 39, no. 6, pp. 1623-1627, Dec. 2009.

[22] U. Engelke, M. Kusuma, H. J. Zepernick, and M. Caldera, "Reduced-reference metric design for objective perceptual quality assessment in wireless imaging", Signal Processing: Image Communication, vol. 24, no. 7, pp. 525-547, Aug. 2009.

[23] Z. Wang, G. Wu, H. R. Sheikh, E. P. Simoncelli, E. Yang, and A. C. Bovik, "Quality-aware images", IEEE Trans. Image Process., vol. 15, no. 6, pp. 1680-1689, Jun. 2006.
[24] Z. Wang, and E. P. Simoncelli, "Reduced-reference image quality assessment using a wavelet-domain natural image statistic model", Proc. SPIE, Human Vision and Electronic Imaging, Jan. 2005.
[25] Q. Li, and Z. Wang, "Reduced-reference image quality assessment using divisive normalization-based image representation", IEEE J. Select. Topics Signal Process., vol. 3, no. 2, pp. 201-211, Apr. 2009.
[26] L. Ma, S. Li, F. Zhang, and K. N. Ngan, "Reduced-reference image quality assessment using reorganized DCT-based image representation", IEEE Trans. Multimedia, vol. 13, no. 4, pp. 824-829, Aug. 2011.
[27] T. M. Cover and J. A. Thomas, "Element of information theory", New York: Wiley, 1991.
[28] Z. Xiong, K. Ramchandran, M. T. Orchard, and Y. Q. Zhang, "A comparative study of DCT- and wavelet-based image coding", IEEE Trans. Circuits Syst. Video Technol., vol. 9, no. 5, pp. 692-695, Aug. 1999.
[29] D. Zhao, W. Gao, and Y. K. Chan, "Morphological representation of DCT coefficients for image compression", IEEE Trans. Circuits Syst. Video Technol., vol. 12, no. 9, pp. 819-823, Sep. 2002.
[30] R. W. Buccigrossi and E. P. Simoncelli, "Image compression via joint statistical characterization in the wavelet domain", IEEE Trans. Image Process., vol. 8, no. 12, pp. 1688-1701, Dec. 1999.
[31] J. Liu and P. Moulin, "Information-theoretic analysis of interscale and intrascale dependencies between image wavelet coefficients", IEEE Trans. Image Process., vol. 10, no. 11, pp. 1647-1658, Nov. 2001.
[32] H. R. Sheikh, Z. Wang, L. Cormack, and A. C. Bovik, LIVE Image Quality Assessment Database. [Online]. Available: http://live.ece.utexas.edu/research/quality.
[33] B. Li, M. R. Peterson, and R. D. Freeman, "Oblique effect: a neural basis in the visual cortex", J. Neurophysiol., pp. 204-217, 2003.
[34] M. N. Do and M. Vetterli, "Wavelet-based texture retrieval using generalized Gaussian density and Kullback-Leibler distance", IEEE Trans. Image Process., vol. 11, no. 2, pp. 146-158, Feb. 2002.
[35] VQEG. Final report from the video quality experts group on the validation of objective models of video quality assessment, 2000. [Online]. Available: http://www.vqeg.org.
[36] H. R. Sheikh, M. F. Sabir, and A. C. Bovik, "A statistical evaluation of recent full reference image quality assessment algorithms", IEEE Trans. Image Process., vol. 15, no. 11, pp. 3440-3451, Nov. 2006.